

MINERAL CHARACTERIZATION OF SOIL TYPE RANKER FORMED ON SERPENTINES OCCURRING IN SOUTHERN BELGRADE ENVIRONS BUBANJ POTOK

by

**Božidar Dj. CEKIĆ¹, Valentin N. IVANOVSKI^{1*}, Aleksandar DJORDJEVIĆ²,
Velimir ALEKSIĆ², Zorica TOMIĆ², Stefan BOGDANOVIĆ³, and Ana B. UMIĆEVIĆ¹**

¹Vinča Institute of Nuclear Sciences, University of Belgrade, Belgrade, Serbia

²Faculty of Agriculture, University of Belgrade, Belgrade, Serbia

³Center for Solid State Physics and New Materials, Institute of Physics,
University of Belgrade, Belgrade, Serbia

Scientific paper

DOI: 10.2298/NTRP1202131C

The paper addresses the issue of health risk associated with the presence of chrysotile in the soil type ranker formed on massive serpentines occurring in the area of Bubanj Potok, a settlement located in the southern Belgrade environs, Serbia. Characterization of the ranker soil was conducted by scanning electron microscopy, X-ray diffraction, micro-Raman spectroscopy and transmission ⁵⁷Fe Mössbauer spectroscopy. Scanning electron microscopy figures showed regular shaped smectite (montmorillonite) particles, aggregates of chlorite, and elongated sheets of serpentines minerals antigorite. X-ray diffraction analysis confirmed the presence of detrital mineral quartz polymorph as well as minor amounts of other mineral species. Micro-Raman spectroscopy identified the presence of dominant minerals, such as montmorillonite, kaolinite, muscovite, gypsum, calcite, albite, amphiboles (hornblende/kaersutite) and orthoclase. Important polymorph silica modifications of quartz, olivine (forsterite), pyroxene (enstatite/ferrosilite, diopside/hedenbergite), and serpentine (antigorite/lizardite/chrysotile) were identified.

Key words: ranker soil, serpentine, chrysotile, Mössbauer spectroscopy, micro-Raman spectroscopy

INTRODUCTION

One of the most widely distributed groups of siliceous rocks in the hilly and mountainous areas of Serbia consists of serpentinitised peridotite rocks. The qualitative and quantitative determination of various serpentine minerals present within massive serpentinites is rather difficult because of their similar structures and chemical compositions [1]. Besides the geodynamical and petrological significance of the precise identification of these minerals, there is a health risk issue associated with the presence of chrysotile or heavy metals. In order to identify the three principal mineral polymorphs of the serpentine group, *i. e.*, chrysotile, lizardite and antigorite, micro-Raman and ⁵⁷Fe Mössbauer spectroscopy were applied in the analysis of the massive serpentines occurring in the Bubanj Potok area, located near Belgrade, Serbia.

Micro-Raman spectroscopy is a non-destructive, rapid technique with no sample preparation, and has the advantage of high spectral resolution and easy data collection in identification of minerals and other

species [2, 3]. ⁵⁷Fe Mössbauer spectroscopy has proved to be a valuable technique in providing information about the characterization of iron minerals in soil and clays [4]. ⁵⁷Fe Mössbauer characterization results in the detection of the iron site geometry, valence state, and co-ordination number, and also provides a quantitative estimate of the iron content of unknown species in a sample. Measured quantities such as the isomer shift (δ), the electric quadrupole splitting (QS) and the hyperfine magnetic field (B), can be used to distinguish between oxidation states of iron in various structural sites and to detect iron oxides of different particle sizes in the investigated sample. The relative amount of each structural state or phase can be obtained with this technique [5, 6].

MATERIALS AND METHODS

The studied site is located in the vicinity of Belgrade in Serbia (20°33'36" Eastern longitude, 44°43'30" Northern latitude, figs. 1 and 2). The soil type ranker formed on serpentine was investigated. Soil samples were collected from nine small-depth profiles, and a single composite sample of A_h soil horizon was formed.

* Corresponding author; e-mail: valiva@vin.bg.ac.rs



Figure 1. The Bubanj Potok location chart

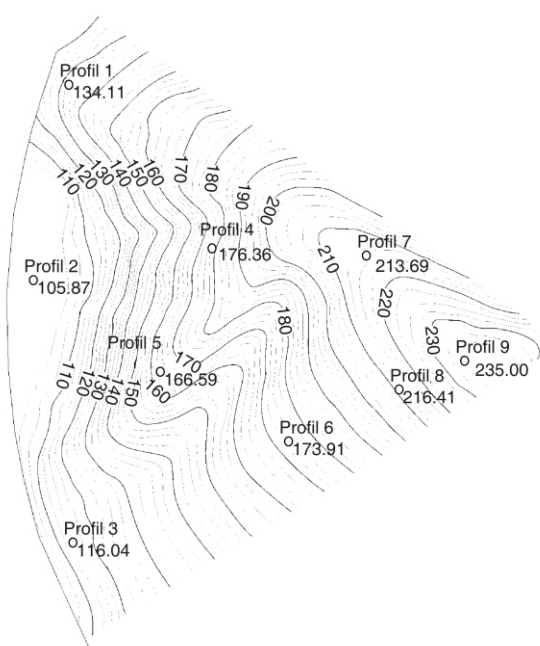


Figure 2. Terrain model – Topographic map with the locations of nine soil profiles of the studied Bubanj Potok soil, ranker type

Scanning electron microscopy (SEM) was done by JEOL Model JSM-6390LV at an accelerated voltage of 15 kV and 20 kV. The specimens were coated with a thin layer of gold (Au) using a Bal-Tec SCD005 Sputter Coater.

A powder X-ray diffraction (XRD) pattern was obtained on the Philips PW1710 powder diffractometer with monochromatic (graphite monochromator) $\text{CuK}\alpha_{1,2}$ radiation ($\lambda = 1.54178 \text{ \AA}^*$). The working voltage and current in the course of data collection were 40 kV and 30 mA, inside $4-70^\circ 2\theta$ range in steps 0.03° , and scanning time of 2s per step. The identification of minerals in total soil and clay fraction of soil was made using the computer program package DRX Win 1.4c.

* $1 \text{ \AA} = 10^{-10} \text{ m}$

The Raman scattering measurements were performed using TriVista 557 Raman system in backscattering micro-Raman configuration. The system was in subtractive mode with 900 g/mm, 900 g/mm, and 2400 g/mm gratings and 200 μm slits. The 514.5 nm line of an Ar^+/Kr^+ mixed gas laser was used as an excitation source. The laser beam focusing was achieved by a long distance microscope objective (magnification 50 times). Laser power on the sample was about 1 mW.

^{57}Fe Mössbauer absorption spectra were obtained in a standard transmission geometry using a source of ^{57}Co in Rh (920 MBq) at room temperature. The spectrometer was operated with a triangular velocity waveform in constant acceleration mode. The measurements were made on a powder sample contained in a plexiglas holder; the surface density of the absorber was 16.7 mg/cm^2 . The data were stored in 1024 multichannel analyzer. The laser spectrum was recorded and fitted in order to recalculate channels in mm/s. The sample thickness corrections were carried out by transmission integral. All quoted isomer shifts (δ) are referred to natural alpha iron at ambient temperature. The spectra were fitted using the WinNormos program created by Brand (2008), using a least squares method [7].

RESULTS AND DISCUSSION

SEM investigation of the Bubanj Potok soil clearly showed the regular-shaped smectite (montmorillonite) particles and aggregates of chlorite, well developed, with different grain sizes (figs. 3 and 4). These aggregates have small deformations on the borders of grains and do not have regular hexagon surfaces. Elongated sheets of lizardite mixed with antigorite were also observed (fig. 4).

Results of semiquantitative XRD analysis of the investigated ranker soil provided limited information on the presence of the following crystal phases: the domi-

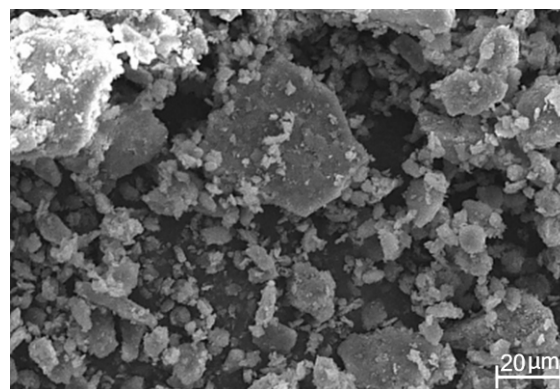


Figure 3. SEM micrograph at magnification 700 of the Bubanj Potok soil sample. Larger single particles indicate smectite phase. Smaller aggregates of particles represent chlorite phase. Marker $20 \mu\text{m}$

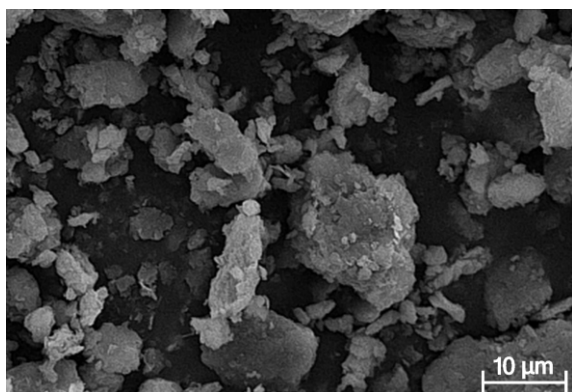


Figure 4. SEM micrograph at magnification 1800 of the Bubanj Potok soil sample. Clay fraction with elongated sheets of lizardite mixed with antigorite. Marker 10 μm

nant detrital mineral quartz polymorph 41%, was identified, along with numerous fractions of minerals in the soil and five oxides up to 59% (fig. 5). The following minor fractions of minerals were present in the soil: interstratifications of chlorite-vermiculite-montmorillonite, chlorite-vermiculite, amphibole (hornblende), talc, muscovite, serpentine-lizardite, quartz polymorph, orthoclase, kaolinite, pyroxenes (enstatite, ferrosilite, diopside and hedenbergite), albite, halosite and montmo-

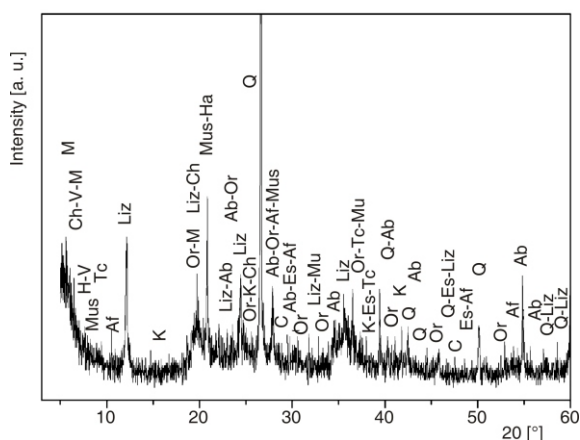


Figure 5. XRD pattern of the Bubanj Potok ranker soil. Present mechanical fractions of minerals in the soil: interstratifications of chlorite-vermiculite-montmorillonite (Ch-V-M), chlorite-vermiculite (Ch-V), amphibole (hornblende) (Af), talc (Tc), muscovite (Mus), serpentine-lizardite (Liz), quartz polymorph (Q), orthoclase (Or), and kaolinite (K); pyroxene (enstatite, ferrosilite, diopside, and hedenbergite) (Es), albite (Ab), halosite (Ha), and montmorillonite (M)

illonite. To assess the productive capacity of the studied ranker soil, the percentage of the five oxides containing Si, Al, Fe, Ca, and Mg were determined by atomic absorption spectrometer (AAS-4000 Perkin-Elmer). Active acidity of the soil, pH in H_2O (1:2.5), was obtained potentiometrically with a pH meter (tab. 1).

Raman spectrum of the Bubanj Potok soil is presented in fig. 6. Raman measurements were done in the range 200-1060 cm^{-1} . Extraction of the data has been performed using a Lorentzian lineshape. The most intense peaks are centered at 465 cm^{-1} (P8), 602 cm^{-1} (P10), and 875 cm^{-1} (P16), whereas groups of less intense peaks are found in the ranges 208-440 cm^{-1} , 520-680 cm^{-1} , and 760-970 cm^{-1} .

The SiO_2 quartz polymorph is characterized by peaks at 354 cm^{-1} (P6), 428 cm^{-1} (P7), 465 cm^{-1} (P8), 813 cm^{-1} (P13), and 836 cm^{-1} (P14), [8-10].

The smectite montmorillonite, was characterized with following peaks: 257 cm^{-1} (P2), 295 cm^{-1} (P3), 875 cm^{-1} (P16), and 916 cm^{-1} (P18), [11]. Raman modes of the end-member Mg-Fe-Ca pyroxenes consist of enstatite: 543 cm^{-1} (P9) and 857 cm^{-1} (P15), ferrosilite: 654 cm^{-1} (P12), diopside: 255 cm^{-1} and hedenbergite: 234 cm^{-1} , [12, 13]. Other minerals present are gypsum ($\text{CaSO}_4 \cdot 2\text{H}_2\text{O}$): 616 cm^{-1} [14], calcite (CaCO_3): 890 cm^{-1} (P17) [14], kaolinite: 335 cm^{-1} (P5), and 918 cm^{-1} (P18) [15, 16], albite: 335 cm^{-1} (P5) and 815 cm^{-1} (P13) [14, 17], mixture of pyroxene and forsterite: 602 cm^{-1} (P10) [14], muscovite: 316 cm^{-1} (P4), [18] silicate amphibole (hornblende): 917 cm^{-1} (P18) [19] and orthoclase: 813 cm^{-1} (P13) [17].

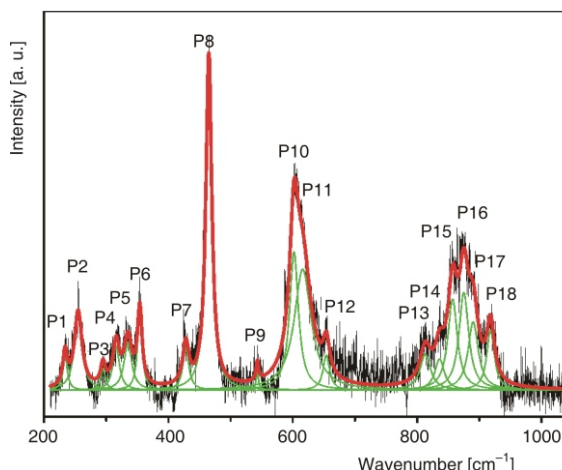


Figure 6. Raman spectrum of the Bubanj Potok soil ranker type. The labeled peaks are explained in the main text

Table 1. Average properties of investigated Bubanj Potok soil, type ranker: chemical composition [%], heat loss [%], and active acidity of the soil, pH in H_2O

Horizon depth [cm]	SiO_2 [%]	Al_2O_3 [%]	Fe_2O_3 [%]	CaO [%]	MgO [%]	Loss in heating [%]	pH in H_2O
A_h (0-20)	46.00(4.33)	5.67(1.61)	20.60(4.39)	0.84(0.25)	7.80(1.61)	20.20(2.89)	6.27(0.06)
(Range)	(41.79-52.21)	(4.12-8.29)	(16.5-27.2)	(0.48-1.11)	(5.98-10.1)	(15.4-24.1)	(6.2-6.36)

The assignment of the Raman peak at 234 cm^{-1} (P1) needs a more careful consideration. The three principal mineral polymorphs of the serpentine group are chrysotile, lizardite and antigorite [20]. Previous experimental results determining the Raman peak within the range of $230\text{--}236\text{ cm}^{-1}$ (P1) suggest that these three serpentine minerals are present [2, 14, 21].

The presence of health-risk chrysotile was investigated by taking the ^{57}Fe Mössbauer absorption spectrum at 294 K of the Bubanj Potok soil (fig. 7). The spectrum consists of one Zeeman sextet and four paramagnetic doublets. The sextet corresponds to the $\gamma\text{-Fe}_2\text{O}_3$, maghemite, in which Fe^{3+} is in octahedral position.

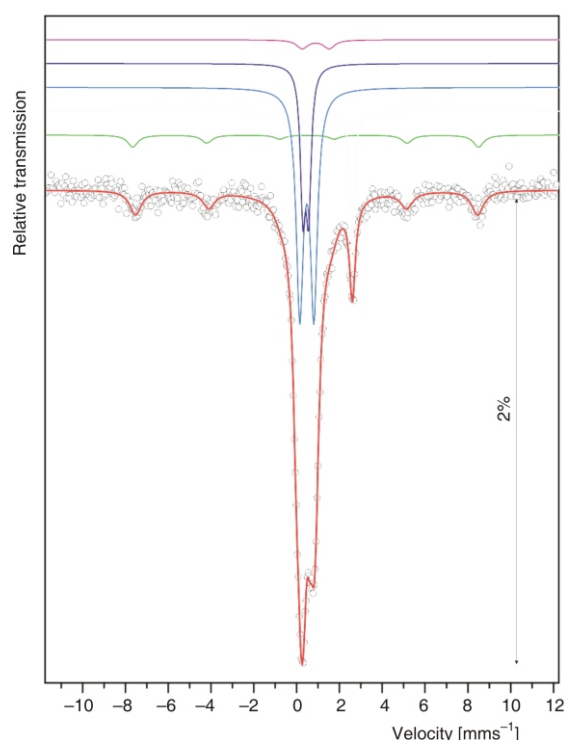


Figure 7. ^{57}Fe Mössbauer absorption spectrum at 294 K of the Bubanj Potok soil ranker type

For the investigated sample, ^{57}Fe Mössbauer data indicate the presence of octahedral Fe^{2+} , octahedral Fe^{3+} and tetrahedral Fe^{3+} (11.2%, 47%, and

14.9% of total iron, respectively) in the present mixed serpentine phases and the presence of octahedral Fe^{3+} (22.2%) in maghemite. The fourth unresolved doublet – $\text{FWHM} = 0.6(3)\text{ mms}^{-1}$ – is presented with 4.7%. The relative contents of the iron containing components were derived from the intensity of the corresponding spectral components omitting the possible influence of the Lamb-Mössbauer factor.

The magnetic phase is observed only in maghemite (tab. 2). The magnetic microstructure of maghemite ($\gamma\text{-Fe}_2\text{O}_3$) is characterized with isomer shift of $0.33(2)\text{ mms}^{-1}$, the magnitude of $50.1(2)\text{ T}$ and negligible quadrupole shift that are in excellent agreement with previously reported data [22, 23]. The three named doublets have origine in serpentine phases [24, 20]. Their Mössbauer parameters are under the influence of presented pyroxenes and amphiboles which are much higher in Fe. The fourth unresolved doublet, characterised with $\delta = 0.8\text{ mms}^{-1}$, and $\text{QS} = 1.3\text{ mms}^{-1}$, appeared as the consequence of undistinguished octahedral positions of Fe^{2+} and Fe^{3+} in pyroxene hedenbergite and amphibole kaersutite [25].

The results of the least squares fit of microcomposites are summarized in tab. 2; the values of isomer shift (δ), quadrupole splitting ($\Delta = eQV_{\text{ZZ}}/2$), hyperfine internal magnetic field (B_{hf}) and area of each component, are reported.

As we have previously shown, the analysis of Bubanj potok soil revealed five oxides with Si, Al, Fe, Ca, and Mg and 18 minerals: quartz, gypsum, calcite, aggregates of chlorite, antigorite, lizardite, montmorillonite, muscovite, kaolinite, albite, forsterite, amphibole (hornblende), orthoclase, four modes of pyroxene (enstatite, ferrosilite, diopside, hedenbergite), including maghemite from analysis of Mössbauer data. The present study indicates that the Bubanj Potok soil is very enriched in silica, with a rough estimation of 41%. The presence of health risk related to chrysotile mineral in the Bubanj Potok soil ranker type, was successfully excluded during the Mössbauer analysis.

ACKNOWLEDGMENT

This work has been partially supported by the Projects ON171001 and ON171032, ON176010, and TR43007, from the Ministry of Education and Science, Republic of Serbia.

Table 2. Selected fit of the ^{57}Fe -Mössbauer parameters for naturally-occurring Fe^{2+} and Fe^{3+} oxides in the Bubanj Potok soil. Site occupancies are marked with (T) for tetrahedral site and (M) for octahedral site

Compound		[mms^{-1}]	QS [mms^{-1}]	B (T)	FWHM [mms^{-1}]	A*
Serpentines	M	1.134	2.68 0.01	50.1 0.2	0.24 0.02	0.112 0.013
	T	0.30 0.02	0.27 0.03		0.28 0.07	0.149 0.052
	M	0.355 0.007	0.66 0.02		0.40 0.03	0.470 0.076
$\gamma\text{-Fe}_2\text{O}_3$		0.33 0.02	0.06 0.05		0.58 0.08	0.222 0.046
Kaersutite/Hedenbergite	M	0.8 0.2	1.3 0.3		0.6 0.3	0.047 0.022

* Relative ration of areas

M – octahedral site

T – tetrahedral site

REFERENCES

- [1] Viti, C., Giacobbe, C., Gualtieri, A. F., Quantitative Determination of Chrysotile in Massive Serpentinities Using DTA: Implication for Asbestos Determinations, *American Mineralogist*, 96 (2011), 7, pp. 1003-1011
- [2] Rinaudo, C., Gastaldi, D., Characterization of Chrysotile, Antigorite and Lizardite by FT-Raman Spectroscopy, *The Canadian Mineralogist*, 41 (2003), 4, pp. 883-890
- [3] Mao, H. K., Hemley, R. J., Chao, E. C. T., The Application of Micro-Raman, Spectroscopy to Analysis and Identification of Minerals in thin Section, *Scanning Microscopy*, 1 (1987), 2, pp. 495-501
- [4] Rancourt, D. G., Mössbauer Spectroscopy in Clay Science, *Hyperfine Interactions*, 117 (1998), 1-4, pp. 3-38
- [5] Vandenberghe, R. E., De Grave, E., Characterization of Goethite and Hematite in a Tunisian Soil Profile by Mössbauer Spectroscopy, *Clays and Clay Minerals*, 34 (1986), 3, pp. 275-280
- [6] Paduani, C., *et al.*, Mineralogical Characterization of Iron-Rich Clayey Soils from the Middle Plateau in the Southern Region of Brazil, *Applied Clay Science*, 42 (2009), 3-4, pp. 559-562
- [7] Brand, R. A., WinNormos Mössbauer Fitting Program, Universität Duisburg, Germany, 2008
- [8] Kingma, K. J., Hemley, R. J., Raman Spectroscopic Study of Microcrystalline Silica, *American Mineralogist*, 79 (1994), 3-4, pp. 269-273
- [9] Gillet, P., Le Cleac'h, A., Madon, M., High-Temperature Raman Spectroscopy of SiO₂ and GeO₂ Polymorphs: Anharmonicity and Thermodynamic Properties at High-Temperatures, *Journal of Geophysical Research*, 95 (1990), B13, pp. 21635-21655
- [10] Klopogge, J. T., Frost, R. L., The Effect of Synthesis Temperature on the FT-Raman and FT-IR Spectra of Saponites, *Vibrational Spectroscopy*, 23 (2000), 1, pp. 119-127
- [11] Frost, R. L., Rintoul, L., Lattice Vibrations of Montmorillonite: an FT Raman and X-Ray Diffraction Study, *Applied Clay Science*, 11 (1996), 2, pp. 171-183
- [12] Huang, E., *et al.*, Spectroscopic Characteristics of Mg-Fe-Ca Pyroxenes, *American Mineralogist*, 85 (2000), 3-4, pp. 473-479
- [13] Cervantes-de la Cruz, K. E., *et al.*, Termometría de Dos Piroxenos en Condros de la Condrita Ordinaria Nuevo Mercurio H5, México, *Revista Mexicana de Ciencias Geológicas*, 27 (2010), 1, pp. 134-147
- [14] Villar, S. E. J., Edwards, H. G. M., Near-Infrared Raman Spectra of Terrestrial Minerals: Relevance for the Remote Analysis of Martian Spectral Signatures, *Vibrational Spectroscopy*, 39 (2005), 1, pp. 88-94
- [15] Johnston, C. T., Sposito G., Birge, R. R., Raman Spectroscopic Study of Kaolinite in Aqueous Suspension, *Clays and Clay Minerals*, 33 (1985), 6, pp. 483-489
- [16] Murad, E., Identification of Minor Amounts of Anatase in Kaolins by Raman Spectroscopy, *American Mineralogist*, 82 (1997), 1-2, pp. 203-206
- [17] Fabel, G. W., *et al.*, Structure of Lunar Glasses by Raman and Soft X-Ray Spectroscopy, *Proc. Lunar Sci. Conf., Geochimica et Cosmochimica Acta*, 1 (1972), 3, pp. 939-951
- [18] Friedrich, F., Spectroscopic Investigations of Delaminated and Intercalated Phyllosilicates, Ph. D. thesis, Bauingenieur-, Geo- und Umweltwissenschaften der Universität Friderician zu Karlsruhe (TH) Germany, 2004, p. 89
- [19] Makreski, P., Jovanovski, G., Gajović, A., Minerals from Macedonia XVII, Vibrational Spectra of Some Common Appearing Amphiboles, *Vibrational Spectroscopy*, 40 (2006), 1, pp. 98-109
- [20] O'Hanley, D. S., Dyar, M. D., The Composition of Chrysotile and its Relationship with Lizardite, *The Canadian Mineralogist*, 36 (1998), 3, pp. 727-739
- [21] Auzende, A. L., *et al.*, High-Pressure Behavior of Serpentine Minerals: a Raman Spectroscopic Study, *Physics and Chemistry of Minerals*, 31 (2004), 5, pp. 269-277
- [22] Murad, E., The Characterization of Soils, Clays, and Clay Firing Products, *Hyperfine Interactions*, 111 (1998), 1-4, pp. 251-259
- [23] Cornell, R. M., Schwertmann, U., The Iron Oxides, Structure, Properties, Reactions, Occurrences and Uses, Wiley-VCH Verlag, Weinheim, Germany, 1996, pp. 120-123
- [24] O'Hanley, D. S., Dyar, M. D., The Composition of Lizardite 1T and the Formation of Magnetite in Serpentinities, *American Mineralogist*, 78 (1993), 3-4, pp. 391-404
- [25] Dyar, M. D., *et al.*, Mössbauer Spectroscopy of Earth and Planetary Materials, *The Annual Review of Earth and Planetary Science*, 34 (2006), pp. 83-125

Received on March 8, 2012

Accepted on March 19, 2012

**Божидар Ђ. ЦЕКИЋ, Валентин Н. ИВАНОВСКИ, Александар ЂОРЂЕВИЋ,
Велимир АЛЕКСИЋ, Зорица ТОМИЋ, Стефан БОГДАНОВИЋ, Ана Б. УМИЋЕВИЋ**

**МИНЕРАЛНА КАРАКТЕРИЗАЦИЈА РАНКЕРА ФОРМИРАНОГ НА
СЕРПЕНТИНИТУ ИЗ ОБЛАСТИ БУБАЊ ПОТОКА ЈУЖНО ОД БЕОГРАДА**

Рад се бави питањем здравственог ризика повезаног са присуством хризотила у ранкеру (тип земљишта) формираном на масивном серпентиниту у области Бубањ Потока, насељу које се налази у јужној околини Београда. Карактеризација ранкера је извршена скенирајућом електронском микроскопијом, рендгенском дифракцијом праха, микро-Раман спектроскопијом и трансмисионом ^{57}Fe Месбауер спектроскопијом. Слике добијене скенирајућим електронским микроскопом показују честице смектита регуларног облика монтморионита, агрегата хлорита и издужене листове серпентинског минерала антигорита. Рендгенска дифракциона анализа потврдила је присуство детритал минерала кварцног полиморфа као и мање количине других минералних врста. Микро-Раман спектроскопија идентификовала је присуство доминантних минерала, као што су монтморионит и каолинит, мусковит, гипс, калцит, албит, амфибол (каерсутит/хорнбленда) и ортоклас. Важни полиморфи силика модификације кварца, оливина (форстерит), пироксена (енстатит, феросилит, хеденбергит, диопсид), и серпентина (антигорит, лизардит, хризотил) су били идентификовани.

Кључне речи: ранкер, серпентинит, хризотил, Месбауерова спектроскопија, микро-Раман спектроскопија
